Taylor & Francis
Taylor & Francis Group

Check for updates

On the curvature and internal stresses in a multilayer strip due to uniform heating, electric field, or hydration

V. A. Lubarda[a] (iD) and M. V. Lubarda[b] (iD)

[a]Department of NanoEngineering, UC San Diego, La Jolla, California, USA; [b]Department of Mechanical and Aerospace Engineering, UC San Diego, La Jolla, California, USA

ABSTRACT

An appealing matrix algorithm for calculating the curvature and internal stresses in isotropic multilayer strips subjected to a uniform temperature change is presented. An explicit representation of the effective stiffness matrix is constructed for any number of layers, which is of central importance in the development of the algorithm. Detailed results are given for bi-, tri-, quadra-, quinta-, and septalayers. Closed-form expressions are deduced for multilayer strips with equal thicknesses and equal elastic moduli of all layers. The algorithm is extended to piezoelectric multilayers subjected to an electric field, and hygromorph multilayers subjected to a uniform change of relative moisture. The presented analysis complements an alternative and more general analysis within the well-known anisotropic lamination theory.

1. Introduction

The objective of this article is to provide an explicit matrix algorithm for the determination of the curvature and internal stresses in a multilayer strip, which consists of n perfectly bonded isotropic layers with different thermoelastic properties, due to a uniform temperature change throughout the strip. With an appropriate change of physical variables, the derived algorithm can also be used to determine the curvature and internal stresses in a piezoelectric multilayer strip due to an electric field and electrostriction effects of the layers, and in a hygromorphic multilayer strip due to the change of relative humidity. The presented analysis is based on an extension of the original bending analysis of bimetalic thermostats by Timoshenko [1], and its subsequent generalization to thermally loaded trilayer and multilayer thermostats by Vasudevan and Johnson [2, 3]. It is also an extension of the analysis of multilayer piezoelectric microactuators by DeVoe and Pisano [4], and the analysis of natural and artificial hygromorphs by Reyssat and Mahadevan [5], and Holstov et al. [6]. The developed matrix algorithm for the determination of curvature and internal stresses is appealing due to its simplicity and its explicit form. As such, it complements the matrix algorithms of the more general analysis of the cross-ply and angle-ply laminates subjected to in-plane and bending loads and/or temperature and moisture change, which are based on the anisotropic elasticity and Kirchhoff assumptions for bending of thin plates [7–16].

There have been numerous publications devoted to various aspects of elastic and inelastic analysis of laminar composites under external mechanical loading, as well as thermal, electric, and hydration effects. An analysis of a thin composite plate made of piezothermoelastic layers subjected to stationary thermal and electric fields was presented by Taucher [17]. Various aspects of

---

CONTACT V. A. Lubarda ✉ vlubarda@ucsd.edu 🖥 Department of NanoEngineering, UC San Diego, La Jolla, CA 92093-0448, USA

the analysis of interfacial stresses in bimetal thermostats and multilayer thin films were addressed by Suhir [18–20]. A composite plate containing piezoceramics on both the upper and bottom surfaces was considered by Shen and Weng [21]. Wong and Wong [22] studied a printed circuit board assembly modeled as a trilayer structure subjected to combined temperature and mechanical loadings, taking into account the axial, shear, and flexural deformation of the interconnects. Tibi et al. [23] presented an analytical and experimental study of the trilayer electro-thermal actuators for thin and soft robotics. Multilayer piezoelectric elements for energy harvesting applications have been discussed by Safaei et al. [24]. Thermally induced deformations and stresses, with an accent on fatigue considerations in the context of electronic packaging design, have been discussed by Dasgupta [25]; additional design aspects of electronic packaging were addressed in the handbook edited by Pecht [26]. Thermo-elastic-viscoplastic study of laminate metal-matrix composites was reported by Avila and Tamma [27], and thermo-elastic-plastic analysis of composite laminated plates under uniform and linearly varying temperature by Sayman and Sayman [28], and Sayman [29]. The extension of the analysis of small-strain electrostriction to elastic dielectrics undergoing large deformation was given by Zhao and Suo [30]. The dynamic analysis of piezothermoelastic laminated plates was presented by Tang and Xu [31]. The edge effects in multilayered panels integrated with piezoelectric actuator and sensor layers under thermal gradient loading were studied by Dhanesh and Santosh Kapuria [32]; for the finite element modeling, see Reddy [33], and for an asymptotic analysis, Cheng and Batra [34]. The hygrothermal analysis of multilayered composite plates by using finite elements was given by Cinefra et al. [35]. The study of the swelling induced bending a functionally graded layer in the range of large deformation was recently reported by Shojaeifard, Bayat, and Baghani [36], where the reference to other related work in this area can be found.

The main contribution of the analysis presented in this article is the matrix algorithm for calculating the curvature and internal stresses in multilayer strips due to thermal loading, piezoelectric effect, or hydration. The development of this algorithm is enabled by the construction of an explicit representation of the effective stiffness matrix $[C]$ of a multilayer strip. The expressions for the curvature, axial forces and bending moments in all layers are derived from $[C]$ by the matrix products with appropriate row and column vectors which account for the geometric and thermoelastic properties of individual layers. This is described in Section 5 of the article. In the preceding Sections 2–4, the results are given for a bilayer, trilayer, and quadralayer strip, which greatly helps the construction of the effective stiffness matrix for a multilayer strip with an arbitrary number of layers (n). The analysis of a multilayer strip with equal thicknesses of all layers, and with the modulus of elasticity of each layer taken to be the average of the actual elastic moduli of all layers, is presented in Section 6. The resulting effective stiffness matrix in this case is dependent only on the number of layers n. The corresponding curvature and stress expressions are derived. The derived results for thermally loaded strips are then extended to piezoelectric multilayer strips subjected to electric field, and to hygromorphic multilayer strips subjected to the change of moisture content.

2. Bilayer strip under uniform temperature change

Figure 1 shows a bilayer strip consisting of two perfectly bonded beams of rectangular cross section with widths b_1 and b_2 and heights h_1 and h_2. The layers are made of isotropic elastic materials with thermoelastic properties ($E_i, \nu_i, \alpha_i, \ i = 1, 2$), where E denotes the modulus of elasticity, ν the Poisson ratio of lateral contraction, and α the coefficient of linear thermal expansion. If the strip is uniformly heated from the initial temperature T_0 to the final temperature $T = T_0 + \Delta T$, the self-equilibrating state of stress sets up in the strip. For example, if $\alpha_1 > \alpha_2$, the layer (1) cannot elongate as it would if it was by itself, because of the constraining effect from the bonded layer (2) with a lower value of α. As a result, the layer (1) is under a compressive longitudinal
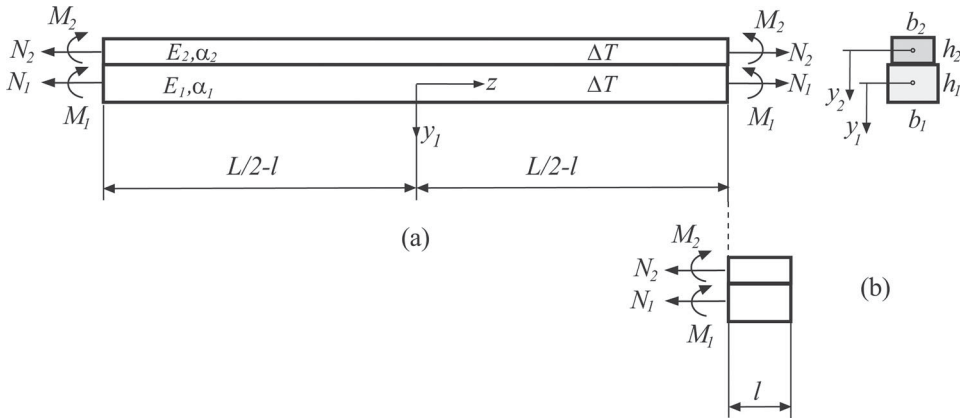
Figure 1. A bilayer strip of length L, made by two bonded layers of rectangular cross sections of dimensions $b_1 \times h_1$ and $b_2 \times h_2$. The moduli of elasticity of two layers are E_1 and E_2, and their coefficients of thermal expansion are α_1 and α_2. The strip is subjected to uniform change of temperature ΔT. (a) At a distance l away from the two ends of the strip (l being approximately equal to the larger side of the cross section of the strip), the layers are under self-equilibrating set of axial forces (N_1, N_2) and bending moments (M_1, M_2). (b) The end of the strip of length l. Its left end is under axial forces (N_1, N_2) and bending moments (M_1, M_2), while its right end is traction free. A multidimensional distribution of stress exist between these two ends.

force, $N_1 = -N$, while the layer (2) is under a tensile force of the same magnitude. The two opposite forces in an arbitrary cross section of the strip (away from the ends of the strip $z = \pm L/2$) constitute a couple of the magnitude $N(h_1 + h_2)/2$. Thus, in order to achieve a self-equilibrating state of stress in the cross section of the strip, the two layers must also carry the internal bending moments M_1 and M_2 (Figure 1a), so that the net bending moment in the cross section of the strip is identically equal to zero. Because of the presence of moments M_1 and M_2, the two layers of the strip bend in the vertical plane, remaining bonded at the interface, such that $M_1 = E_1 I_1 / \rho_1$ and $M_2 = E_2 I_2 / \rho_2$, where ρ_1 is the radius of curvature of the longitudinal centroidal axis of the layer (1), and $\rho_2 = \rho_1 - (h_1 + h_2)/2$ is the radius of curvature of the longitudinal centroidal axis of the layer (2). The bending stiffnesses of the layers are $E_1 I_1$ and $E_2 I_2$, where $I_i = b_i h_i^3 / 12 (i = 1, 2)$. The Euler–Bernoulli assumption is adopted that plane cross-sections of the strip remain plane and are perpendicular to the curved axis of the strip. Since small deformations of the strip are considered, the radii of curvature are much larger than the height of the strip $h_1 + h_2$, and we adopt the approximation $\rho_2 \approx \rho_1 = \rho$ (ρ being loosely referred to as the radius of curvature of the strip), so that the moment-curvature relations are

$$M_1 = E_1 I_1 \, \frac{1}{\rho}, \quad M_2 = E_2 I_2 \, \frac{1}{\rho}. \tag{2.1}$$

The net longitudinal force in each cross section of the strip must vanish, $N_1 + N_2 = 0$, while the condition for the vanishing net moment in the cross section of the strip is

$$M_1 + M_2 + N_1 \, \frac{h_1 + h_2}{2} = 0. \tag{2.2}$$

To complete the set of equations for determining the unknown quantities $(\rho, N_1, N_2, M_1, M_2)$, one imposes the bonded interface condition which requires that the longitudinal strain along the interface is the same for both layers, i.e.,

$$\alpha_1 \Delta T + \frac{N_1}{E_1 A_1} - \frac{h_1}{2\rho} = \alpha_2 \Delta T + \frac{N_2}{E_2 A_2} + \frac{h_2}{2\rho}, \tag{2.3}$$

where $A_i = b_i h_i (i = 1, 2)$ are the cross-sectional areas of the layers. The curvature is assumed to be concave upward (for the opposite, concave downward curvature, the radius ρ would be formally negative). By substituting $N_2 = -N_1$ into (2.3), we obtain

$$N_1 = \frac{c_1 c_2}{c} \left[(\alpha_2 - \alpha_1)\Delta T + (h_1 + h_2) \, \frac{1}{2\rho} \right], \tag{2.4}$$

where $c_1 = E_1 A_1$, $c_2 = E_2 A_2$, and $c = c_1 + c_2$. In an approximate strength-of-materials type of analysis, we do not require the continuity of the lateral strain along the interface in the direction within the cross section of the strip, which would require the consideration of Poisson's ratio of two layers and multidimensional stress analysis. For long strips, this omission is not significantly affecting the accuracy of the longitudinal internal stresses, orthogonal to the cross section of the strip, obtained from a simplified analysis. If the widths of the layers are much larger than their thicknesses, the plane strain approximation in the direction of the width (away from its ends) has been adopted in some work, in which case the same analysis applies with the replacement of E_i with $E_i/(1 - \nu_i^2)$ and α_i with $\alpha_i(1 + \nu_i)$ [4]. If the width is comparable to the length, a configuration of a thin rectangular plate is obtained with equal biaxial state of stress at the points of each layer, and two equal curvatures of the deformed (spherical) shape of the plate. In this case E_i is replaced with $E_i/(1 - \nu_i)$, while α_i remains unchanged [1].

To determine the curvature $1/\rho$, we substitute (2.1) and (2.4) into (2.2). This gives the expression originally derived (for $b_1 = b_2$) by Timoshenko (op. cit.), which, for the latter comparison with thermal loading of multilayer strips, we write as

$$\frac{1}{\rho} = \frac{2p}{q} \, \Delta T, \tag{2.5}$$

where

$$p = c_1 c_2 (h_1 + h_2)(\alpha_1 - \alpha_2), \quad q = 4ck + c_1 c_2 (h_1 + h_2)^2, \tag{2.6}$$

and

$$k_1 = E_1 I_1, \quad k_2 = E_2 I_2, \quad k = k_1 + k_2 = (c_1 h_1^2 + c_2 h_2^2)/12. \tag{2.7}$$

An equivalent expression for $b_1 \neq b_2$ was originally given by Chu, Mehregany, and Mullen [37].

The force N_1 follows by substitution of (2.5) into (2.4),

$$N_1 = 4c_1 c_2 k \, \frac{\alpha_2 - \alpha_1}{4ck + c_1 c_2 (h_1 + h_2)^2} \, \Delta T, \quad N_2 = -N_1, \tag{2.8}$$

while the moments M_1 and M_2 follow from (2.1) and (2.5) as

$$\begin{aligned}
M_1 &= k_1 \, \frac{1}{\rho} = 2k_1 \, \frac{p}{q} \, \Delta T = \frac{2k_1 c_1 c_2 (h_1 + h_2)(\alpha_1 - \alpha_2)}{4ck + c_1 c_2 (h_1 + h_2)^2} \, \Delta T, \\
M_2 &= k_2 \, \frac{1}{\rho} = 2k_2 \, \frac{p}{q} \, \Delta T = \frac{2k_2 c_1 c_2 (h_1 + h_2)(\alpha_1 - \alpha_2)}{4ck + c_1 c_2 (h_1 + h_2)^2} \, \Delta T.
\end{aligned} \tag{2.9}$$

Having determined (N_1, N_2) and (M_1, M_2), the longitudinal stresses in two layers are determined from simple beam formulas

$$\sigma_i = \frac{N_i}{A_i} + \frac{M_i}{I_i} \, y_i, \quad (i = 1, 2), \tag{2.10}$$

where y_1 and y_2 are the vertical coordinates from the centroids of the cross sections of two layers, measured positive downwards.

The stress state near the traction-free ends of the strip $z = \pm L/2$ (Figure 1a) is multidimensional and cannot be determined in closed form, but away from these ends, by the Saint-Venant's principle, expressions (2.10) predict the stress state sufficiently accurately. Note that neither curvature nor stresses depend on b in the case of a bilayer strip of uniform width ($b_1 = b_2 = b$). The analytical and numerical analysis of stresses near the ends of thermally loaded strips, particularly shorter strips, which includes the determination of the shear and normal stresses along the
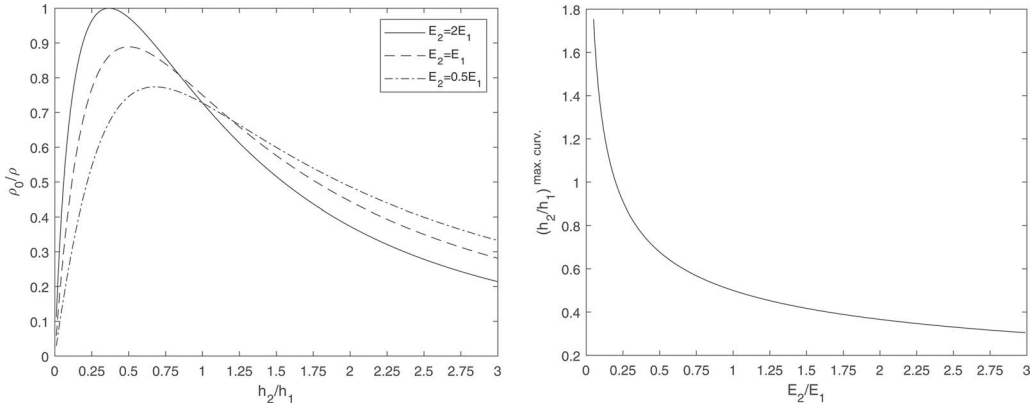
Figure 2. (a) The normalized curvature ρ_0/ρ vs. the thickness ratio h_2/h_1. The normalizing factor is $1/\rho_0 = (\alpha_1 - \alpha_2)\Delta T/h_1$. (b) The thickness ratio $(h_2/h_1)^{\text{max.curv.}}$ which maximizes the curvature $1/\rho$ versus the elastic moduli ratio E_2/E_1.

interface, is of great importance for the study of interface strength and prevention of interface cracking. The references in this regard, mostly in the context of layered electronic structures, include Chen and Nelson [38], Chen, Cheng and Gerhardt [39], Suhir [18–20], Suo and Hutchinson [40], Jiang et al. [41], Xie and Sitaraman [42], and Wen and Basaran [43]. Lee and Jasiuk [44] investigated the asymptotic behavior of stresses at the interface near the edge of two semi-infinite bimaterial strips under constant temperature change.

It may be of design interest to determine for which thickness ratio $\eta = h_2/h_1$ the radius of curvature is maximized in the case $b_1 = b_2$, given the elastic moduli ratio $e = E_2/E_1$ and thermal expansion coefficients α_1 and α_2. Applying the stationary condition to (2.5) it readily follows that this thickness ratio is the positive real root of the quintic polynomial

$$2e^2\eta^5 + (4 + 3e)e\eta^4 + 8e\eta^3 + 2e\eta^2 - 2\eta - 1 = 0. \tag{2.11}$$

For example, if $E_2 = 2E_1$, the curvature is maximized if the second layer has the thickness $h_2 = 0.366h_1$; if $E_2 = E_1$ the thickness is $h_2 = 0.5h_1$, while $h_2 = h_1$ for $E_2 = 0.2E_1$. The normalized curvature is plotted versus the thickness ratio h_2/h_1, for the three selected values of E_2/E_1, in Figure 2a. Figure 2b shows the plot of the curvature maximizers $(h_2/h_1)^{\text{max.curv.}}$ versus the elastic moduli ratio E_2/E_1. For each pair of elastic moduli (E_1, E_2), the corresponding values of thermal expansion (α_1, α_2) are assumed to be given. For bimetallic termostats, the copper/steel or brass/steel layers are often used. The thermoelastic properties in this case are $(E_{\text{Cu}} = 117 \text{ GPa},$ $\alpha_{\text{Cu}} = 1.7 \times 10^{-5} \text{ K}^{-1})$, $(E_{\text{brass}} = 97 \text{ GPa}, \alpha_{\text{brass}} = 1.9 \times 10^{-5} \text{ K}^{-1})$, $(E_{\text{steel}} = 180 \text{ GPa},$ $\alpha_{\text{steel}} = 1.3 \times 10^{-5} \text{ K}^{-1})$. In the case of copper/steel bimetallic strip $(E_2/E_1 = E_{\text{steel}}/E_{\text{Cu}} = 1.5385)$ it readily follows that maximum curvature is obtained for $h_{\text{steel}} = 0.412 \, h_{\text{Cu}}$, while in the case of brass/steel bimetallic strip $(E_2/E_1 = E_{\text{steel}}/E_{\text{brass}} = 1.8557)$ the maximum curvature is obtained for $h_{\text{steel}} = 0.379 \, h_{\text{brass}}$. If the temperature change is $\Delta T = 100$ K, the corresponding radii of curvature are $\rho = 2,607 \, h_{\text{Cu}}$ and $\rho = 1,686 \, h_{\text{brass}}$. If the length of a strip is L, the maximum deflection in the middle of the strip, relative to the ends of the strip, is $v_{\text{max}} = L^2/8\rho$ (ignoring the end effects). One can also proceed to optimize the value of h_2 by minimizing the maximum stress in a bimetallic strip.

3. Trilayer strip

Figure 3 shows a strip made of three bonded layers. Away from their ends, the layers are under internal forces and moments produced by a uniform temperature change ΔT throughout the strip. The governing equations in each cross section of the strip are
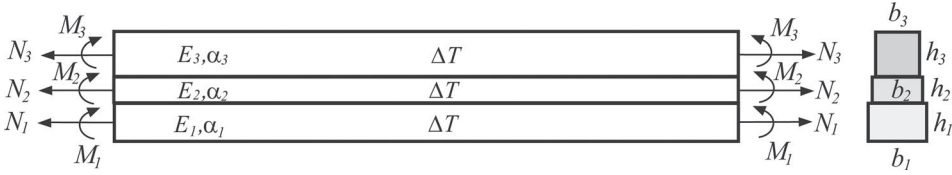
Figure 3. A trilayer strip made of three bonded layers of rectangular cross sections of dimensions $b_1 \times h_1$, $b_2 \times h_2$, and $b_3 \times h_3$. The moduli of elasticity of three layers are E_1, E_2, and E_2, and their coefficients of thermal expansion are α_1, α_2, and α_3. The strip is subjected to uniform change of temperature ΔT. Away from the ends of the strip, the layers are under axial forces (N_1, N_2, N_3) and bending moments (M_1, M_2, M_3), which are self-equilibrating in each cross section of the strip.

$$N_1 + N_2 + N_3 = 0, \tag{3.1}$$

$$M_1 + M_2 + M_3 + N_1 \, \frac{h_1 + 2h_2 + h_3}{2} + N_2 \, \frac{h_2 + h_3}{2} = 0. \tag{3.2}$$

The interface conditions for equal longitudinal strains between the layers along two interfaces are

$$\alpha_1 \Delta T + \frac{N_1}{E_1 A_1} - \frac{h_1}{2\rho} = \alpha_2 \Delta T + \frac{N_2}{E_2 A_2} + \frac{h_2}{2\rho},$$
$$\alpha_2 \Delta T + \frac{N_2}{E_2 A_2} - \frac{h_2}{2\rho} = \alpha_3 \Delta T - \frac{N_1 + N_2}{E_3 A_3} + \frac{h_3}{2\rho}, \tag{3.3}$$

where $N_3 = -(N_1 + N_2)$ was used on the right-hand side of the second expression in (3.3). The moment-curvature relations are

$$M_i = k_i \frac{1}{\rho}, \quad k_i = E_i I_i, \quad (i = 1, 2, 3). \tag{3.4}$$

To proceed, it is convenient to cast the analysis in matrix form and, thus, we rewrite (3.3) as

$$\begin{bmatrix} \dfrac{1}{c_1} & -\dfrac{1}{c_2} \\[2mm] \dfrac{1}{c_3} & \dfrac{1}{c_2} + \dfrac{1}{c_3} \end{bmatrix} \cdot \left\{ \begin{array}{c} N_1 \\ N_2 \end{array} \right\} = \left\{ \begin{array}{c} \alpha_2 - \alpha_1 \\ \alpha_3 - \alpha_2 \end{array} \right\} \Delta T + \left\{ \begin{array}{c} h_1 + h_2 \\ h_2 + h_3 \end{array} \right\} \frac{1}{2\rho}, \tag{3.5}$$

where $c_i = E_i A_i (i = 1, 2, 3)$ are the axial stiffnesses of the layers. The matrix

$$[D] = \begin{bmatrix} \dfrac{1}{c_1} & -\dfrac{1}{c_2} \\[2mm] \dfrac{1}{c_3} & \dfrac{1}{c_2} + \dfrac{1}{c_3} \end{bmatrix} \tag{3.6}$$

can be viewed as an effective axial compliance matrix of the strip. Its inverse, the effective axial stiffness matrix, is

$$[C] = [D]^{-1} = \frac{1}{c} \begin{bmatrix} c_1(c_2 + c_3) & c_1 c_3 \\[2mm] -c_1 c_2 & c_2 c_3 \end{bmatrix}, \quad c = c_1 + c_2 + c_3. \tag{3.7}$$

Thus, from (3.5), it follows that

$$\left\{ \begin{array}{c} N_1 \\ N_2 \end{array} \right\} = [C] \cdot \left\{ \begin{array}{c} \alpha_2 - \alpha_1 \\ \alpha_3 - \alpha_2 \end{array} \right\} \Delta T + [C] \cdot \left\{ \begin{array}{c} h_1 + h_2 \\ h_2 + h_3 \end{array} \right\} \frac{1}{2\rho}. \tag{3.8}$$

On the other hand, by substituting (3.4) into (3.2), we obtain

$$k \frac{1}{\rho} + \frac{1}{2} \begin{bmatrix} h_1 + 2h_2 + h_3 & h_2 + h_3 \end{bmatrix} \cdot \begin{Bmatrix} N_1 \\ N_2 \end{Bmatrix} = 0, \tag{3.9}$$

where $k = k_1 + k_2 + k_3$. After using (3.8) in (3.9), this becomes

$$\left(k + \frac{1}{4} \begin{bmatrix} h_1 + 2h_2 + h_3 & h_2 + h_3 \end{bmatrix} \cdot [C] \cdot \begin{Bmatrix} h_1 + h_2 \\ h_2 + h_3 \end{Bmatrix} \right) \frac{1}{\rho}$$

$$= \frac{1}{2} \begin{bmatrix} h_1 + 2h_2 + h_3 & h_2 + h_3 \end{bmatrix} \cdot [C] \cdot \begin{Bmatrix} \alpha_1 - \alpha_2 \\ \alpha_2 - \alpha_3 \end{Bmatrix} \Delta T. \tag{3.10}$$

Upon using (3.7) for the matrix $[C]$ and performing the needed matrix products, the following expression for the curvature is obtained,

$$\frac{1}{\rho} = \frac{2p}{q} \Delta T, \tag{3.11}$$

where

$$p = c_1[(c_2 + c_3)(h_1 + h_2) + c_3(h_2 + h_3)](\alpha_1 - \alpha_2) + c_3[c_1(h_1 + h_2) + (c_1 + c_2)(h_2 + h_3)](\alpha_2 - \alpha_3), \tag{3.12}$$

$$q = 4ck + c_1(c_2 + c_3)(h_1 + h_2)^2 + c_3(c_1 + c_2)(h_2 + h_3)^2 + 2c_1c_3(h_1 + h_2)(h_2 + h_3). \tag{3.13}$$

Expression (3.11), with p and q defined by (3.12) and (3.13), represents an explicit trilayer strip generalization of Timoshenko's expression (2.5) for a thermally loaded bilayer strip. An equivalent expression, in terms of the ratio of two four-by-four determinants, was obtained by Vasudevan and Johnson [2] by applying the Cramer's rule to the system of four linear algebraic equations for four unknowns $(P_1, P_2, P_3, 1/\rho)$.

The forces N_1 and N_2 follow by substituting (3.11) into (3.8). This gives

$$\begin{Bmatrix} N_1 \\ N_2 \end{Bmatrix} = [C] \cdot \begin{Bmatrix} \alpha_2 - \alpha_1 + \dfrac{p}{q} (h_1 + h_2) \\ \alpha_3 - \alpha_2 + \dfrac{p}{q} (h_2 + h_3) \end{Bmatrix} \Delta T, \tag{3.14}$$

i.e., after using (3.7) for the matrix $[C]$,

$$N_1 = \frac{c_1}{c} \left\{ (c_2 + c_3) \left[\alpha_2 - \alpha_1 + \frac{p}{q} (h_1 + h_2) \right] + c_3 \left[\alpha_3 - \alpha_2 + \frac{p}{q} (h_2 + h_3) \right] \right\} \Delta T, \tag{3.15}$$

$$N_2 = \frac{c_2}{c} \left\{ -c_1 \left[\alpha_2 - \alpha_1 + \frac{p}{q} (h_1 + h_2) \right] + c_3 \left[\alpha_3 - \alpha_2 + \frac{p}{q} (h_2 + h_3) \right] \right\} \Delta T. \tag{3.16}$$

The moments follow from (3.4) by using (3.11) and are given by

$$M_i = 2k_i \frac{p}{q} \Delta T, \quad k_i = E_i I_i, \quad (i = 1, 2, 3). \tag{3.17}$$

The stresses in the layers are

$$\sigma_i = \frac{N_i}{A_i} + \frac{M_i}{I_i} y_i, \quad (i = 1, 2, 3), \tag{3.18}$$

where y_1, y_2, and y_3 are the vertical coordinates from the centroids of the cross sections of the three layers, measured positive downwards.

If a trilayer is symmetric ($E_1 = E_3$, $\alpha_1 = \alpha_3$, $h_1 = h_3$), it readily follows from (3.12) that $p = 0$, i.e., there is no curvature and bending stresses in a symmetric strip loaded by uniform temperature change ($1/\rho = 0$, $M_i = 0$ for $i = 1, 2, 3$). The normal stress is entirely due to normal forces, which are, from (3.15) and (3.16),

$$N_1 = N_3 = -\frac{c_1 c_2}{c}\,(\alpha_1 - \alpha_2), \quad N_2 = \frac{2 c_1 c_2}{c}\,(\alpha_1 - \alpha_2), \quad c = 2c_1 + c_2. \tag{3.19}$$

4. Quadralayer strip

For the strip of four bonded layers, the governing equilibrium equations are

$$N_1 + N_2 + N_3 + N_4 = 0, \tag{4.1}$$

$$M_1 + M_2 + M_3 + M_4 + N_1\,\frac{h_1 + 2(h_2 + h_3) + h_4}{2} + N_2\,\frac{h_2 + 2h_3 + h_4}{2} + N_3\,\frac{h_3 + h_4}{2} = 0. \tag{4.2}$$

Since the moment-curvature relations are

$$M_i = k_i\,\frac{1}{\rho}, \quad k_i = E_i I_i, \quad (i = 1, 2, 3, 4), \tag{4.3}$$

Equation (4.2) can be written in the matrix form as

$$k\,\frac{1}{\rho} = -\frac{1}{2}\big[\,h_1 + 2(h_2 + h_3) + h_4 \quad h_2 + 2h_3 + h_4 \quad h_3 + h_4\,\big] \cdot \left\{ \begin{array}{c} N_1 \\ N_2 \\ N_3 \end{array} \right\}, \quad k = \sum_{i=1}^{4} k_i. \tag{4.4}$$

The interface conditions for equal longitudinal strains between the layers along three interfaces, expressed in the matrix form and incorporating the relationship $N_4 = -(N_1 + N_2 + N_3)$, are

$$\begin{bmatrix} \dfrac{1}{c_1} & -\dfrac{1}{c_2} & 0 \\[2mm] 0 & \dfrac{1}{c_2} & -\dfrac{1}{c_3} \\[2mm] \dfrac{1}{c_4} & \dfrac{1}{c_4} & \dfrac{1}{c_3} + \dfrac{1}{c_4} \end{bmatrix} \cdot \left\{ \begin{array}{c} N_1 \\ N_2 \\ N_3 \end{array} \right\} = \left\{ \begin{array}{c} \alpha_2 - \alpha_1 \\ \alpha_3 - \alpha_2 \\ \alpha_4 - \alpha_3 \end{array} \right\} \Delta T + \left\{ \begin{array}{c} h_1 + h_2 \\ h_2 + h_3 \\ h_3 + h_4 \end{array} \right\} \frac{1}{2\rho}, \tag{4.5}$$

where $c_i = E_i A_i (i = 1, 2, 3, 4)$. It can be readily shown that the inverse of the axial compliance matrix

$$[D] = \begin{bmatrix} \dfrac{1}{c_1} & -\dfrac{1}{c_2} & 0 \\[2mm] 0 & \dfrac{1}{c_2} & -\dfrac{1}{c_3} \\[2mm] \dfrac{1}{c_4} & \dfrac{1}{c_4} & \dfrac{1}{c_3} + \dfrac{1}{c_4} \end{bmatrix} \tag{4.6}$$

is

$$[C] = [D]^{-1} = \frac{1}{c} \begin{bmatrix} c_1(c_2 + c_3 + c_4) & c_1(c_3 + c_4) & c_1 c_4 \\[2mm] -c_1 c_2 & c_2(c_3 + c_4) & c_2 c_4 \\[2mm] -c_1 c_3 & -c_3(c_1 + c_2) & c_3 c_4 \end{bmatrix}, \quad c = \sum_{i=1}^{4} c_i. \tag{4.7}$$

Thus, from (4.5), it follows that

$$\begin{Bmatrix} N_1 \\ N_2 \\ N_3 \end{Bmatrix} = [C] \cdot \begin{Bmatrix} \alpha_2 - \alpha_1 \\ \alpha_3 - \alpha_2 \\ \alpha_4 - \alpha_3 \end{Bmatrix} \Delta T + [C] \cdot \begin{Bmatrix} h_1 + h_2 \\ h_2 + h_3 \\ h_3 + h_4 \end{Bmatrix} \frac{1}{2\rho}. \tag{4.8}$$

By substituting this into the curvature expression (4.4), we obtain

$$\left(k + \frac{1}{4} \begin{bmatrix} h_1 + 2(h_2 + h_3) + h_4 & h_2 + 2h_3 + h_4 & h_3 + h_4 \end{bmatrix} \cdot [C] \cdot \begin{Bmatrix} h_1 + h_2 \\ h_2 + h_3 \\ h_3 + h_4 \end{Bmatrix} \right) \frac{1}{\rho}$$

$$= \frac{1}{2} \begin{bmatrix} h_1 + 2(h_2 + h_3) + h_4 & h_2 + 2h_3 + h_4 & h_3 + h_4 \end{bmatrix} \cdot [C] \cdot \begin{Bmatrix} \alpha_1 - \alpha_2 \\ \alpha_2 - \alpha_3 \\ \alpha_3 - \alpha_4 \end{Bmatrix} \Delta T. \tag{4.9}$$

Consequently, the curvature of a quadralayer strip under uniform temperature change ΔT is

$$\frac{1}{\rho} = \frac{2p}{q} \, \Delta T, \tag{4.10}$$

where

$$p = c \begin{bmatrix} h_1 + 2(h_2 + h_3) + h_4 & h_2 + 2h_3 + h_4 & h_3 + h_4 \end{bmatrix} \cdot [C] \cdot \begin{Bmatrix} \alpha_1 - \alpha_2 \\ \alpha_2 - \alpha_3 \\ \alpha_3 - \alpha_4 \end{Bmatrix}, \tag{4.11}$$

$$q = 4kc + c \begin{bmatrix} h_1 + 2(h_2 + h_3) + h_4 & h_2 + 2h_3 + h_4 & h_3 + h_4 \end{bmatrix} \cdot [C] \cdot \begin{Bmatrix} h_1 + h_2 \\ h_2 + h_3 \\ h_3 + h_4 \end{Bmatrix}. \tag{4.12}$$

The forces N_1 and N_2 follow by substituting (4.10) into (4.8), which gives

$$\begin{Bmatrix} N_1 \\ \\ N_2 \\ \\ N_3 \end{Bmatrix} = [C] \cdot \begin{Bmatrix} \alpha_2 - \alpha_1 + \dfrac{p}{q} \, (h_1 + h_2) \\ \\ \alpha_3 - \alpha_2 + \dfrac{p}{q} \, (h_2 + h_3) \\ \\ \alpha_4 - \alpha_3 + \dfrac{p}{q} \, (h_3 + h_4) \end{Bmatrix} \Delta T. \tag{4.13}$$

The moments and stresses are then obtained from expressions (3.17) and (3.18), with $i = 1, 2, 3, 4$.

5. Multilayer strip

The governing equations for a multilayer strip with n bonded layers are straightforward generalizations of Eqs. (4.1)–(4.5). By the same analysis as used for bi-, tri-, and quadralyer strips in Sections 2–4, it follows that the curvature of the strip under uniform temperature change ΔT is

$$\frac{1}{\rho} = \frac{2p}{q} \, \Delta T, \tag{5.1}$$

where

$$p = c \left[h_1 + 2\sum_{i=2}^{n-1} h_i + h_n \quad h_2 + 2\sum_{i=3}^{n-1} h_i + h_n \quad \ldots \quad h_{n-2} + 2h_{n-1} + h_n \quad h_{n-1} + h_n \right] \cdot [C] \cdot \left\{ \begin{array}{c} \alpha_1 - \alpha_2 \\ \alpha_2 - \alpha_3 \\ \vdots \\ \alpha_{n-2} - \alpha_{n-1} \\ \alpha_{n-1} - \alpha_n \end{array} \right\},$$

(5.2)

$$q = 4kc + c \left[h_1 + 2\sum_{i=2}^{n-1} h_i + h_n \quad h_2 + 2\sum_{i=3}^{n-1} h_i + h_n \quad \ldots \quad h_{n-2} + 2h_{n-1} + h_n \quad h_{n-1} + h_n \right] \cdot [C] \cdot \left\{ \begin{array}{c} h_1 + h_2 \\ h_2 + h_3 \\ \vdots \\ h_{n-2} + h_{n-1} \\ h_{n-1} + h_n \end{array} \right\}, \quad (5.3)$$

with $c_i = E_i A_i (i = 1, 2, \ldots n)$ and $c = \sum_{i=1}^{n} c_i$.

The axial forces in the first $(n - 1)$ layers are

$$\left\{ \begin{array}{c} N_1 \\ N_2 \\ \vdots \\ N_{n-2} \\ N_{n-1} \end{array} \right\} = [C] \cdot \left\{ \begin{array}{c} \alpha_2 - \alpha_1 + \dfrac{p}{q}(h_1 + h_2) \\ \alpha_3 - \alpha_2 + \dfrac{p}{q}(h_2 + h_3) \\ \vdots \\ \alpha_{n-1} - \alpha_{n-2} + \dfrac{p}{q}(h_{n-2} + h_{n-1}) \\ \alpha_n - \alpha_{n-1} + \dfrac{p}{q}(h_{n-1} + h_n) \end{array} \right\} \Delta T.$$

(5.4)

The axial force in the remaining n^{th} layer is $N_n = -\sum_{i=1}^{n-1} N_i$. Finally, the moments in the layers are

$$M_i = 2k_i \frac{p}{q} \Delta T, \quad k_i = E_i I_i, \quad (i = 1, 2, \ldots, n), \qquad (5.5)$$

while the stresses are

$$\sigma_i = \frac{N_i}{A_i} + \frac{M_i}{I_i} y_i, \quad (i = 1, 2, \ldots, n), \qquad (5.6)$$

where $y_i (i = 1, 2, \ldots, n)$ are the vertical coordinates from the centroids of the cross sections of the layers, measured positive downwards. If all layers are of the same width b, the curvature and stresses are independent of b, while the forces N_i and moments M_i scale with b. An alternative but computationally less appealing expression for the curvature was given in terms of the ratio of two determinants of the dimension $(n + 1) \times (n + 1)$ by Vasudevan and Johnson [3], which was derived by applying the Cramer's rule to the system of $(n + 1)$ linear algebraic equations for $(n + 1)$ unknowns $(N_1, N_2, \ldots, N_n, 1/\rho)$.

The effective stiffness matrix $[C]$ appearing in (5.2)–(5.4) is the inverse of the effective compliance matrix

$$
[D] = \begin{bmatrix}
\dfrac{1}{c_1} & -\dfrac{1}{c_2} & 0 & 0 & \cdots & 0 & 0 & 0 \\[2mm]
0 & \dfrac{1}{c_2} & -\dfrac{1}{c_3} & 0 & \cdots & 0 & 0 & 0 \\[2mm]
0 & 0 & \dfrac{1}{c_3} & -\dfrac{1}{c_4} & \cdots & 0 & 0 & 0 \\[2mm]
\vdots & \vdots & \vdots & \vdots & \vdots & \vdots & \vdots & \vdots \\[2mm]
0 & 0 & 0 & 0 & \cdots & \dfrac{1}{c_{n-3}} & -\dfrac{1}{c_{n-2}} & 0 \\[2mm]
0 & 0 & 0 & 0 & \cdots & 0 & \dfrac{1}{c_{n-2}} & -\dfrac{1}{c_{n-1}} \\[2mm]
\dfrac{1}{c_n} & \dfrac{1}{c_n} & \dfrac{1}{c_n} & \dfrac{1}{c_n} & \cdots & \dfrac{1}{c_n} & \dfrac{1}{c_n} & \dfrac{1}{c_{n-1}}+\dfrac{1}{c_n}
\end{bmatrix}. \tag{5.7}
$$

This form of the matrix $[D]$ is similar, but not identical, to the matrix $[A]$ used in the analysis of piezoelectric cantilever microactuators by DeVoe and Pisano [4].

5.1. Effective stiffness matrix

Based on the derived results for trilayer and quadralayer strips, it can be recognized by inspection that the diagonal elements of the effective stiffness matrix $[C] = [D]^{-1}$ for an arbitrary n are defined by

$$
c_{kk} = \frac{c_k}{c} \sum_{i=k+1}^{n} c_i, \quad k = 1, 2, \ldots, n-1. \tag{5.8}
$$

The off-diagonal elements above the main diagonal of the matrix are

$$
c_{kl} = \frac{c_k}{c} \sum_{i=l+1}^{n} c_i, \quad k = 1, 2, \ldots, n-2, \quad l = k+1, k+2, \ldots, n-1 \quad (k < l), \tag{5.9}
$$

while the off-diagonal elements below the main diagonal are

$$
c_{kl} = -\frac{c_k}{c} \sum_{i=1}^{l} c_i, \quad k = 2, 3, \ldots, n-1, \quad l = 1, 2, \ldots, k-1 \quad (l < k). \tag{5.10}
$$

To gain more insight about the structure of the effective stiffness matrix $[C]$ for a multilayer strip, we list below its explicit form for a quinta-, sexta-, and septalayer strip.

Quintalayer strip:

$$
[C] = \frac{1}{c} \begin{bmatrix}
c_1 \displaystyle\sum_{i=2}^{5} c_i & c_1 \displaystyle\sum_{i=3}^{5} c_i & c_1(c_4 + c_5) & c_1 c_5 \\[3mm]
-c_2 c_1 & c_2 \displaystyle\sum_{i=3}^{5} c_i & c_2(c_4 + c_5) & c_2 c_5 \\[3mm]
-c_3 c_1 & -c_3(c_1 + c_2) & c_3(c_4 + c_5) & c_3 c_5 \\[3mm]
-c_4 c_1 & -c_4(c_1 + c_2) & -c_4 \displaystyle\sum_{i=1}^{3} c_i & c_4 c_5
\end{bmatrix}, \quad c = \sum_{i=1}^{5} c_i. \tag{5.11}
$$

Sextalayer strip:

$$[C] = \frac{1}{c} \begin{bmatrix} c_1 \sum_{i=2}^{6} c_i & c_1 \sum_{i=3}^{6} c_i & c_1 \sum_{i=4}^{6} c_i & c_1(c_5 + c_6) & c_1 c_6 \\ -c_2 c_1 & c_2 \sum_{i=3}^{6} c_i & c_2 \sum_{i=4}^{6} c_i & c_2(c_5 + c_6) & c_2 c_6 \\ -c_3 c_1 & -c_3(c_1 + c_2) & c_3 \sum_{i=4}^{6} c_i & c_3(c_5 + c_6) & c_3 c_6 \\ -c_4 c_1 & -c_4(c_1 + c_2) & -c_4 \sum_{i=1}^{3} c_i & c_4(c_5 + c_6) & c_4 c_6 \\ -c_5 c_1 & -c_5(c_1 + c_2) & -c_5 \sum_{i=1}^{3} c_i & -c_5 \sum_{i=1}^{4} c_i & c_5 c_6 \end{bmatrix}, \quad c = \sum_{i=1}^{6} c_i. \quad (5.12)$$

Septalayer strip:

$$[C] = \frac{1}{c} \begin{bmatrix} c_1 \sum_{i=2}^{7} c_i & c_1 \sum_{i=3}^{7} c_i & c_1 \sum_{i=4}^{7} c_i & c_1 \sum_{i=5}^{7} c_i & c_1(c_6 + c_7) & c_1 c_7 \\ -c_2 c_1 & c_2 \sum_{i=3}^{7} c_i & c_2 \sum_{i=4}^{7} c_i & c_2 \sum_{i=5}^{7} c_i & c_2(c_6 + c_7) & c_2 c_7 \\ -c_3 c_1 & -c_3(c_1 + c_2) & c_3 \sum_{i=4}^{7} c_i & c_3 \sum_{i=5}^{7} c_i & c_3(c_6 + c_7) & c_3 c_7 \\ -c_4 c_1 & -c_4(c_1 + c_2) & -c_4 \sum_{i=1}^{3} c_i & c_4 \sum_{i=5}^{7} c_i & c_4(c_6 + c_7) & c_4 c_7 \\ -c_5 c_1 & -c_5(c_1 + c_2) & -c_5 \sum_{i=1}^{3} c_i & -c_5 \sum_{i=1}^{4} c_i & c_5(c_6 + c_7) & c_5 c_7 \\ -c_6 c_1 & -c_6(c_1 + c_2) & -c_6 \sum_{i=1}^{3} c_i & -c_6 \sum_{i=1}^{4} c_i & -c_6 \sum_{i=1}^{5} c_i & c_6 c_7 \end{bmatrix}, \quad c = \sum_{i=1}^{7} c_i. \quad (5.13)$$

6. Multilayers with uniform thickness and modulus of elasticity

An appealing special case for which the results simplify considerably is the case when all layers have the same width b and the same thickness $h_1 = h_2 = \cdots = h_n = h/n$, where h is the total height of the strip, and when the moduli of elasticity of individual layers are not very different from each other (for example, aluminum has $E = 69$ GPa and $\alpha_1 = 2.4 \times 10^{-5}$ $^\circ$C^{-1}, while silver has $E = 72$ GPa and $\alpha_1 = 1.8 \times 10^{-5}$ $^\circ$C^{-1}), so that a homogenization assumption can be adopted by which all layers have the same modulus of elasticity, which is equal to the average modulus of elasticity $E = (E_1 + E_2 + \cdots + E_n)/n$. This is a good simplifying assumption because the differences in the coefficient of thermal expansion are in this case a dominant driving force for the strip curvature and the corresponding bending stresses. From (5.8) to (5.10) it then readily follows that the effective stiffness matrix is

$$[C] = \frac{Ebh}{n^2} [C_0], \quad [C_0] =
\begin{bmatrix}
n-1 & n-2 & n-3 & n-4 & \cdots & 4 & 3 & 2 & 1 \\
-1 & n-2 & n-3 & n-4 & \cdots & 4 & 3 & 2 & 1 \\
-1 & -2 & n-3 & n-4 & \cdots & 4 & 3 & 2 & 1 \\
-1 & -2 & -3 & n-4 & \cdots & 4 & 3 & 2 & 1 \\
\vdots & \vdots & \vdots & \vdots & \vdots & \vdots & \vdots & \vdots \\
-1 & -2 & -3 & -4 & \cdots & -(n-4) & 3 & 2 & 1 \\
-1 & -2 & -3 & -4 & \cdots & -(n-4) & -(n-3) & 2 & 1 \\
-1 & -2 & -3 & -4 & \cdots & -(n-4) & -(n-3) & -(n-2) & 1
\end{bmatrix}, \quad (6.1)$$

where $c_i = Ebh/n (i = 1, 2, ..., n)$ and $c = Ebh$, Furthermore, $k_i = (Eb/12)(h/n)^3$ $(i = 1, 2, ..., n)$, $k = (Eb/12)h^3/n^2$, and, from (5.2)–(5.3), we obtain

$$p = \frac{E^2 b^2 h^3}{n^2} [\mathbb{N}] \cdot
\begin{Bmatrix}
\alpha_1 - \alpha_2 \\
\alpha_2 - \alpha_3 \\
\vdots \\
\alpha_{n-2} - \alpha_{n-1} \\
\alpha_{n-1} - \alpha_n
\end{Bmatrix}, \quad (6.2)$$

$$q = \frac{E^2 b^2 h^4}{3n^2} + \frac{2E^2 b^2 h^4}{n^3} [\mathbb{N}] \cdot
\begin{Bmatrix}
1 \\
1 \\
\vdots \\
1 \\
1
\end{Bmatrix}. \quad (6.3)$$

A row vector $[\mathbb{N}]$ is obtained from

$$[\mathbb{N}] = \frac{2}{n} \begin{bmatrix} n-1 & n-2 & \cdots & 2 & 1 \end{bmatrix} \cdot [C_0]. \quad (6.4)$$

It turns out that the value of q in (6.3) is independent of n, because, for any value of n, (6.3) reduces to

$$q = \frac{1}{3} E^2 b^2 h^4. \quad (6.5)$$

Thus, by substituting (6.2) and (6.5) into the curvature expression (5.1) it follows that

$$\frac{1}{\rho} = \frac{6\Delta T}{n^2 h} [\mathbb{N}] \cdot
\begin{Bmatrix}
\alpha_1 - \alpha_2 \\
\alpha_2 - \alpha_3 \\
\vdots \\
\alpha_{n-2} - \alpha_{n-1} \\
\alpha_{n-1} - \alpha_n
\end{Bmatrix}. \quad (6.6)$$

After performing the matrix product in (6.4), the row vector $[\mathbb{N}]$ for even number of layers n takes the form

$$[\mathbb{N}] = \left[n-1 \ \ 2(n-2) \ \ 3(n-3) \ \ ... \ \ \frac{n^2}{4}-1 \ \ \frac{n^2}{4} \ \ \frac{n^2}{4}-1 \ \ ... \ \ 3(n-3) \ \ 2(n-2) \ \ n-1\right], \qquad (6.7)$$

while, for odd n,

$$[\mathbb{N}] = \left[n-1 \ \ 2(n-2) \ \ 3(n-3) \ \ ... \ \ \frac{n^2-9}{4} \ \ \frac{n^2-1}{4} \ \ \frac{n^2-1}{4} \ \ \frac{n^2-9}{4} \ \ ... \ \ 3(n-3) \ \ 2(n-2) \ \ n-1\right]. \qquad (6.8)$$

The terms appearing in the middle part of $[\mathbb{N}]$ in (6.7) and (6.8) are obtained from

$$\frac{n^2}{4}-1 = \left(\frac{n}{2}-1\right)\left[n-\left(\frac{n}{2}-1\right)\right], \quad \frac{n^2}{4} = \frac{n}{2}\left(n-\frac{n}{2}\right),$$

$$\frac{n^2-9}{4} = \left(\frac{n-1}{2}-1\right)\left[n-\left(\frac{n-1}{2}-1\right)\right], \quad \frac{n^2-1}{4} = \frac{n-1}{2}\left(n-\frac{n-1}{2}\right).$$

For example, for the values of $n = 2, ..., 10$, the row vector $[\mathbb{N}]$ is

$$[\mathbb{N}] = \begin{cases} [1], & n=2, \\ [2 \quad 2], & n=3, \\ [3 \quad 4 \quad 3], & n=4, \\ [4 \quad 6 \quad 6 \quad 4], & n=5, \\ [5 \quad 8 \quad 9 \quad 8 \quad 5], & n=6, \\ [6 \quad 10 \quad 12 \quad 12 \quad 10 \quad 6], & n=7, \\ [7 \quad 12 \quad 15 \quad 16 \quad 15 \quad 12 \quad 7], & n=8, \\ [8 \quad 14 \quad 18 \quad 20 \quad 20 \quad 18 \quad 14 \quad 8], & n=9, \\ [9 \quad 16 \quad 21 \quad 24 \quad 25 \quad 24 \quad 21 \quad 16 \quad 9], & n=10. \end{cases} \qquad (6.9)$$

Consequently, for a bilayer strip ($n = 2$), the curvature is

$$\frac{1}{\rho} = \frac{3\Delta T}{2h} \ (\alpha_1 - \alpha_2), \qquad (6.10)$$

as in Timoshenko [1], while for trilayer and quadralyer strips

$$\frac{1}{\rho} = \frac{\Delta T}{h} \begin{cases} \dfrac{4}{3} \ (\alpha_1 - \alpha_3), & n=3, \\ \dfrac{3}{8} \ [3(\alpha_1 - \alpha_4) + (\alpha_2 - \alpha_3)], & n=4, \end{cases} \qquad (6.11)$$

as in Vasudevan and Johnson [3]. For quinta, sexta, septa and octalayers, the curvature is

$$\frac{1}{\rho} = \frac{\Delta T}{h} \begin{cases} \dfrac{12}{25} \ [2(\alpha_1 - \alpha_5) + (\alpha_2 - \alpha_4)], & n=5, \\[2mm] \dfrac{1}{6} \ [5(\alpha_1 - \alpha_6) + 3(\alpha_2 - \alpha_5) + (\alpha_3 - \alpha_4)], & n=6, \\[2mm] \dfrac{12}{49} \ [3(\alpha_1 - \alpha_7) + 2(\alpha_2 - \alpha_6) + (\alpha_3 - \alpha_5)], & n=7, \\[2mm] \dfrac{3}{32} \ [7(\alpha_1 - \alpha_8) + 5(\alpha_2 - \alpha_7) + 3(\alpha_3 - \alpha_6) + (\alpha_4 - \alpha_5)], & n=8. \end{cases} \qquad (6.12)$$

It can be recognized from these expressions that in order to produce the largest (positive) curvature of the strip, the layers should be sequenced with the values of their thermal expansion coefficients in the descending order from the bottom to the top of the multilayer strip.

6.1. Stress expressions

Since bending stiffnesses of all layers are equal to each other, $k_i = E_i I_i = (1/12)Eb(h/n)^3$, the bending moments in all layers are also equal to each other, and given by

$$M_i = \frac{k_i}{\rho} = \frac{Ebh^3}{12n^3\rho}, \quad (i = 1, 2, ..., n), \tag{6.13}$$

with ρ determined from (6.6). The axial forces follow from (5.4),

$$\begin{Bmatrix} N_1 \\ N_2 \\ \vdots \\ N_{n-2} \\ N_{n-1} \end{Bmatrix} = \frac{Ebh}{n^2} \, [C_0] \cdot \begin{Bmatrix} (\alpha_2 - \alpha_1)\Delta T + \dfrac{h}{n\rho} \\ (\alpha_3 - \alpha_2)\Delta T + \dfrac{h}{n\rho} \\ \vdots \\ (\alpha_{n-1} - \alpha_{n-2})\Delta T + \dfrac{h}{n\rho} \\ (\alpha_n - \alpha_{n-1})\Delta T + \dfrac{h}{n\rho} \end{Bmatrix}, \tag{6.14}$$

with $[C_0]$ given in (6.1).

For example, in the case $n = 3$ we obtain

$$\begin{Bmatrix} N_1 \\ N_2 \\ N_3 \end{Bmatrix} = \frac{Ebh}{27} \begin{Bmatrix} -2\alpha_1 + 3\alpha_2 - \alpha_3 \\ 3\alpha_1 - 6\alpha_2 + 3\alpha_3 \\ -\alpha_1 + 3\alpha_2 - 2\alpha_3 \end{Bmatrix} \Delta T, \quad M_1 = M_2 = M_3 = \frac{Ebh^2}{243}(\alpha_1 - \alpha_3)\Delta T. \tag{6.15}$$

The corresponding stresses at the bottom ($y_i = -h/6$) and the top ($y_i = h/6$) of each layer follow from (5.6),

$$\begin{Bmatrix} \sigma_1 \\ \sigma_2 \\ \sigma_3 \end{Bmatrix}_{\text{bott}} = \frac{E\Delta T}{9} \begin{Bmatrix} 3\alpha_2 - 3\alpha_3 \\ 5\alpha_1 - 6\alpha_2 + \alpha_3 \\ \alpha_1 + 3\alpha_2 - 4\alpha_3 \end{Bmatrix}, \quad \begin{Bmatrix} \sigma_1 \\ \sigma_2 \\ \sigma_3 \end{Bmatrix}_{\text{top}} = \frac{E\Delta T}{9} \begin{Bmatrix} -4\alpha_1 + 3\alpha_2 + \alpha_3 \\ \alpha_1 - 6\alpha_2 + 5\alpha_3 \\ -3\alpha_1 + 3\alpha_2 \end{Bmatrix}. \tag{6.16}$$

The stress discontinuities at two interfaces are

$$\sigma_2^{\text{bott}} - \sigma_1^{\text{top}} = E\Delta T(\alpha_1 - \alpha_2), \quad \sigma_3^{\text{bott}} - \sigma_2^{\text{top}} = E\Delta T(\alpha_2 - \alpha_3). \tag{6.17}$$

Recalling that in the case of a bilayer strip the stress discontinuity at the interface is $\sigma_2^{\text{bott}} - \sigma_1^{\text{top}} = E\Delta T(\alpha_1 - \alpha_2)$, we recognize that the stress discontinuities at $(n-1)$ interfaces of a multilayer strip with n layers are

$$\sigma_{i+1}^{\text{bott}} - \sigma_i^{\text{top}} = E\Delta T(\alpha_i - \alpha_{i+1}), \quad (i = 1, 2, ...n - 1). \tag{6.18}$$

Thus, the stress discontinuity at the interface between two layers depends only on the difference of the thermal expansion coefficients of the two neighboring layers (and $E\Delta T$), independently of the values of the thermal expansion coefficients of other layers. Physically, this could have been recognized from the outset, because, in the case of uniform modulus of elasticity, there cannot be any stress discontinuity across the interface between two layers of equal thermal expansion coefficient, regardless of the values of thermal expansion coefficients in other layers.

7. Piezoelectric multilayers subjected to electric field

The analysis presented for thermally loaded multilayer strips and the derived results can be readily extended to piezoelectric multilayers subjected to electric field. In this case, the longitudinal thermal strain in the ith layer $\epsilon_{zz}^{i,\text{thermal}} = \alpha_i \Delta T$ is replaced with piezoelectric strain $\epsilon_{zz}^{i,\text{piezo}} = d_i \mathcal{E}_i$, where d_i stands for the transverse piezoelectric coupling coefficient for the strain in the z direction due to the electric field $\mathcal{E}_i$ applied across the thickness of the layer i in the y direction (commonly denoted in the literature as d_{yz}^i or d_{31}^i). The negative value of d_i indicates contraction. If a layer is not piezoelectric, the coefficient d_i for that layer is equal to zero. Also, if some layers in the strip are conductors, their static electric field is zero. The electric field in the ith layer can be expressed in terms of the applied voltage (voltage drop across the entire multilayer strip, ΔV) as

$$\mathcal{E}_i = \frac{\Delta V_i}{h_i} = \frac{\Delta V/\kappa_i}{\sum_{j=1}^n h_j/\kappa_j}, \quad \Delta V_i = \frac{h_i/\kappa_i}{\sum_{j=1}^n h_j/\kappa_j} \, \Delta V, \tag{7.1}$$

where κ_i is the dielectric constant of the ith layer. Thus, the piezoelectric strain becomes

$$\epsilon_{zz}^{i,\text{piezo}} = d_i \mathcal{E}_i = \beta_i \Delta V, \quad \beta_i = \frac{d_i/\kappa_i}{\sum_{j=1}^n h_j/\kappa_j}. \tag{7.2}$$

Consequently, the curvature of a piezoelectric multilayer strip can be determined from an expression analogous to (5.1),

$$\frac{1}{\rho} = \frac{2p}{q} \, \Delta V, \tag{7.3}$$

i.e., by replacing ΔT in (5.1) by ΔV, and the column vector of the differences of thermal expansion coefficients α_i in the expression (5.2) for p by the column vector of the differences of piezoelectric parameters β_i, as shown below

$$\left\{ \begin{array}{c} \alpha_1 - \alpha_2 \\ \alpha_2 - \alpha_3 \\ \vdots \\ \alpha_{n-2} - \alpha_{n-1} \\ \alpha_{n-1} - \alpha_n \end{array} \right\} \mapsto \left\{ \begin{array}{c} \beta_1 - \beta_2 \\ \beta_2 - \beta_3 \\ \vdots \\ \beta_{n-2} - \beta_{n-1} \\ \beta_{n-1} - \beta_n \end{array} \right\}. \tag{7.4}$$

The stiffness matrix $[C]$ remains the same as given in Section 5 for a thermally loaded multilayer strip, as well as the row vector containing the heights of the layers. Furthermore, the parameter q appearing in (7.1) is the same for both the thermally loaded multilayer strip and the piezoelectric multilayer strip under electric field. This analysis of curvature and resulting stresses in a piezoelectric multilayer strip due to applied voltage generalizes the analysis of DeVoe and Pisano [4], who assumed that d_{31} is the same for all piezoelectric layers, which may be of interest for the design of piezoactuators and energy harvesting devices, and for other MEMS applications.

For example, for a bilayer strip with piezoelectric layer (1) and metallic layer (2), the curvature is

$$\frac{1}{\rho} = \frac{2c_1 c_2 (h_1 + h_2) d_1}{4ck + c_1 c_2 (h_1 + h_2)^2} \frac{\Delta V}{h_1}, \tag{7.5}$$

as in DeVoe and Pisano [4], and, for $b_1 = b_2$, Smits and Choi [45]. For a quadralayer strip with its second layer being piezoelectric ($d_1 = d_3 = d_4 = 0$), from (5.2) the parameter p becomes

$$p = \beta_2 c_2 [c_2 (h_2 + 2h_3 + h_4) + c_3 (h_2 + h_3) - c_1 (h_1 + h_2)]. \tag{7.6}$$

If the average modulus of elasticity (E) is used for all layers of the same width b, (7.6) simplifies to

$$p = \beta_2 E^2 b^2 h_2 (h_2^2 + h_3^2 - h_1^2 + h_2 h_4 + 3h_2 h_3 - h_1 h_2). \tag{7.7}$$

Furthermore, if all layers are of the same thickness, equal to $h/4$, (7.7) reduces to $p = \beta_2 E^2 b^2 h^3/16$. Thus, since in this case, from (6.5), the parameter $q = E^2 b^2 h^3/3$, the curvature (7.3) becomes

$$\frac{1}{\rho} = \frac{3\beta_2}{8h} \Delta V, \quad \beta_2 = \frac{d_2/\kappa_2}{\sum_{j=1}^4 h_j/\kappa_j} \tag{7.8}$$

This result also follows directly from the piezoelectric analogue of the second expression in (6.11) by replacing there ΔT with ΔV, α_2 with β_2, and α_1, α_3 and α_4 with zero. If the layers 1, 3, and 4 are conductors, then their dielectric constants are infinite, the parameter $\beta_2 = d_2/h_2$, and (7.8) reduces to

$$\frac{1}{\rho} = \frac{3d_2}{2h^2} \Delta V. \tag{7.9}$$

For a piezoelectric layer with $d_2 = -5$ pC/N (for ZnO film, the reported value in the literature for d_{31} is -4.7 pC/N), from (7.9) it follows that in order to produce the radius of curvature $\rho \approx 5 \times 10^5 \ h$ the applied voltage needs to be $\Delta V = 1$ V for the strip of thickness $h = 4 \ \mu$ m, and $\Delta V = 1$ kV for the strip of thickness $h = 4$ mm. If $d_2 = -100$ pC/N (for PZT film, the reported value of d_{31} is -105 pC/N), the applied voltage $\Delta V = 1$ V would produce the radius of curvature $\rho \approx 2.5 \times 10^4 \ h$ for the strip of thickness $h = 4 \ \mu$ m, while $\Delta V = 1$ kV would be needed to produce the curvature $\rho \approx 2.5 \times 10^4 \ h$ for the strip of thickness $h = 4$ mm. The negative values of ρ indicate that the curvature is concave downward, as expected because the piezoelectric layer is placed in the lower part of the strip and the utilized values of d_{31} are negative.

8. Hygromorphic multilayers under uniform change of hydration

The theory of hygrothermoelasticity is discussed by Sih et al. [46]. A comprehensive hygrothermal laminate analysis can be found in Herakovich [8], Tsai and Hahn [14], and Vasiliev and Morozov [15]. For a hygromorphic multilayer strip with different coefficients of hygroexpansion (γ_i) in different layers, subjected to uniform change of the moisture content (hydration change, ΔH) in the entire strip, the hygromorphic strain in the ith layer is $\epsilon_{zz}^{i,\text{hygro}} = \gamma_i \Delta H$. For a dry state, the parameter $H = 0$, while for a fully hydrated state $H = 1$. Consequently, all results derived for a thermally loaded multilayer strip from Sections 2 to 6 apply in this case by replacing ΔT with ΔH, and α_i with γ_i. For example, the curvature of a trilayer strip, with equal widths of all layers, is, from (3.11) to (3.13),

$$\frac{1}{\rho} = \frac{2p}{q} \Delta H, \tag{8.1}$$

where

$$p = E_1 h_1 [(E_2 h_2 + E_3 h_3)(h_1 + h_2) + E_3 h_3 (h_2 + h_3)](\gamma_1 - \gamma_2) \\ + E_3 h_3 [E_1 h_1 (h_1 + h_2) + (E_1 h_1 + E_2 h_2)(h_2 + h_3)](\gamma_2 - \gamma_3), \tag{8.2}$$

$$q = \frac{1}{3} \ (E_1 h_1 + E_2 h_2 + E_3 h_3)(E_1 h_1^3 + E_2 h_2^3 + E_3 h_3^3) + E_1 h_1 (E_2 h_2 + E_3 h_3)(h_1 + h_2)^2 \\ + E_3 h_3 (E_1 h_1 + E_2 h_2)(h_2 + h_3)^2 + 2E_1 h_1 E_3 h_3 (h_1 + h_2)(h_2 + h_3). \tag{8.3}$$

The forces, moments, and stresses in the layers follow from the analogues of (5.4)–(5.6).

If the outer layers are of the same material ($E_1 = E_3 \neq E_2$, $\gamma_1 = \gamma_3 \neq \gamma_2$), and $h_1 = h_2$, the objective may be to determine the thickness ratio h_3/h_2 which maximizes the curvature $1/\rho$, for
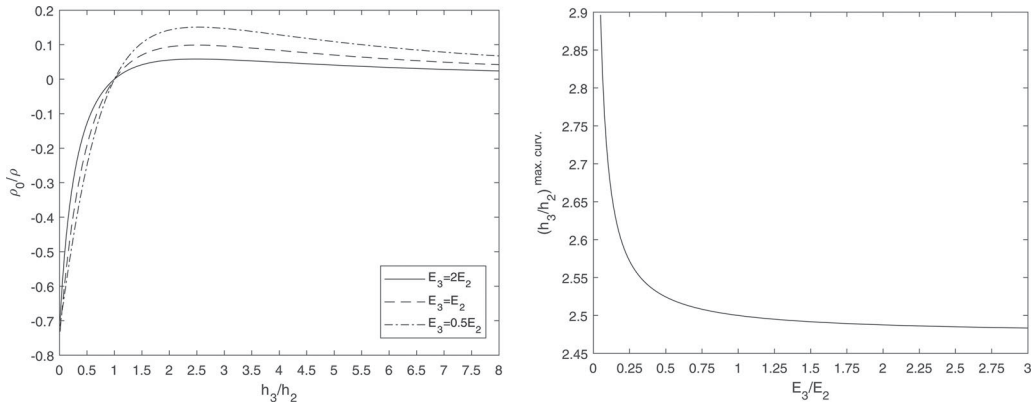
Figure 4 (a) The normalized curvature ρ_0/ρ vs. the thickness ratio h_3/h_2. The normalizing factor is $1/\rho_0 = (\gamma_2 - \gamma_3)\Delta H/h_2$. (b) The thickness ratio $(h_3/h_2)^{\text{max.curv.}}$ which maximizes the curvature $1/\rho$ versus the elastic moduli ratio E_3/E_2.

given values of (E_1, E_2), (γ_1, γ_2), and $h_1 = h_2$. From (8.1) to (8.3), it follows that in this case the expression for the normalized curvature is

$$\frac{\rho_0}{\rho} = \frac{6e(\eta^2 + \eta - 2)}{1 + 2e(2\eta^3 + 3\eta^2 + 2\eta + 7) + e^2(\eta^4 + 4\eta^3 + 18\eta^2 + 28\eta + 1)}, \quad \frac{1}{\rho_0} = \frac{(\gamma_2 - \gamma_3)\Delta H}{h_2} \quad (8.4)$$

where $e = E_3/E_2$ and $\eta = h_3/h_2$. Applying the stationary condition to (8.4), it follows that the thickness ratio $e = h_3/h_2$ which maximizes the curvature is the positive real root of the quintic polynomial

$$2e^2\eta^5 + (4 + 7e)e\eta^4 + 8e\eta^3 - 2e(11 + 17e)\eta^2 - 2(1 + 26\eta + 37e^2) - (1 + 22e + 57e^2) = 0. \quad (8.5)$$

The normalized curvature is plotted versus the thickness ratio h_3/h_2, for the three selected values of E_3/E_2, in Figure 4a. If $h_3 = h_2$, the trilayer strip is symmetric and the curvature is equal to zero. Figure 4b shows the plot of the curvature maximizers $(h_3/h_2)^{\text{max.curv.}}$ versus the elastic moduli ratio E_3/E_2.

Other design considerations may be of interest. For example, in the study of the hydration-induced deformation of the pine cone by Quan et al. [47], the material and geometric parameters are such that $h_1 = h_3$ and $\gamma_1 = \gamma_2$, while $E_2 \ll (E_1, E_3)$. In this case, the curvature expressions become approximately, but very accurately,

$$\frac{1}{\rho} = \frac{12(\gamma_1 - \gamma_3)\Delta H}{h_1} \frac{1 + h_2/h_1}{12(1 + h_2/h_1)^2 + (1 + e)^2/e}, \quad e = \frac{E_3}{E_1}. \quad (8.6)$$

Using the numerical values from the cited reference (*ibid.*), $h_1 = h_3 = 1.5$ mm, $h_2 = 0.8$ mm, $E_1 = 0.86$ GPa, $E_2 = 0.09$ GPa, $E_3 = 4.53$ GPa, $\gamma_1 = \gamma_2 = 0.2$, $\gamma_3 = 0.06$, expression (8.6) gives $1/\rho = 48.14 \, \Delta H$ (m^{-1}). If the hydration change from the reference state is $\Delta H = 0.2$, the radius of curvature is $\rho = 103.85$ mm. The expressions (8.1)–(8.3) give $\rho = 102.6$ mm. The corresponding normal forces and bending moments, per common width b of the layers, from expressions of the form (3.15)–(3.17), are $\{N_1, N_2, N_3\}/b = \{-5.87, \ -1.13, 7.00\}$ (N/mm), and $\{M_1, M_2, M_3\}/b = \{2.36, \ 0.037, 12.42\}$ (N).

9. Conclusions

An explicit matrix algorithm for calculating the curvature and internal stresses in isotropic multilayer strips subjected to a uniform temperature change is developed and presented. Of central importance in the development of this algorithm is the explicit representation of the effective

stiffness matrix $[C]$, for any number of layers n. Detailed results are given for bi-, tri-, quadra-, quinta-, and septalayers. Closed-form expressions for curvature and stresses are deduced for the multilayer strips with equal thicknesses and equal elastic moduli of all layers. The derived results, of interest for structural mechanics applications including the study of thermally-induced buckling, complements the more general and well-known analysis of anisotropic lamination theory. The obtained results for thermally loaded multilayer strips are extended to piezoelectric multilayers under applied voltage, and hygromorphic multilayers subjected to a uniform change of moisture content, which are of interest for the design of piezoelectric and hygromorphic actuators and other devices of MEMS and bioengineering technology, and they may also be of interest for the analysis of magnetostrictive thin films exhibiting large magnetostriction [48–56].

An alternative appealing approach to the analysis of isotropic multilayer strips, in the spirit of the present work, is to develop recursive formulas by which the curvature and stresses in a multilayer strip with n layers are expressed in terms of the curvature and stresses in a multilayer strip with $n-1$ layers. The development of such formulas is presented in our accompanying article [57].

Acknowledgments

ORCID

V. A. Lubarda http://orcid.org/0000-0002-0474-6681
M. V. Lubarda http://orcid.org/0000-0002-3755-271X

References

[1] S. Timoshenko, "Analysis of bi-metal thermostats," *J. Opt. Soc. Am*, vol. 11, no. 3, pp. 233–256, 1925. DOI: 10.1364/JOSA.11.000233.
[2] M. Vasudevan and W. Johnson, "Thermal bending of a tri-metal strip," *J. R. Aeronaut. Soc*, vol. 65, no. 607, pp. 507–509, 1961a. DOI: 10.1017/S0368393100074976.
[3] M. Vasudevan and W. Johnson, "On multi-metal thermostats," *Appl. Sci. Res*, vol. 9, no. 6, pp. 420–430, 1961b. DOI: 10.1007/BF02921840.
[4] D. L. DeVoe and A. P. Pisano, "Modeling and optimal design of piezoelectric cantilever microactuators," *J. Microelectromech. Syst.*, vol. 6, no. 3, pp. 266–270, 1997. DOI: 10.1109/84.623116.
[5] E. Reyssat and L. Mahadevan, "Hygromorphs: From pine cones to biomimetic bilayers," *J. R. Soc Interface*, vol. 6, no. 39, pp. 951–957, 2009. DOI: 10.1098/rsif.2009.0184.
[6] A. Holstov, B. Bridgens and G. Farmer, "Hygromorphic materials for sustainable responsive architecture," *Constr. Build. Mater*, vol. 98, pp. 570–582, 2015. DOI: 10.1016/j.conbuildmat.2015.08.136.
[7] R. M. Christensen, 1991, *Mechanics of Composite Materials*. Krieger Publ., Malabar, FL.
[8] C. T. Herakovich, 1998, *Mechanics of Fibrous Composite*. Wiley, New York.
[9] R. M. Jones, 1999, *Mechanics of Composites Materials* (2nd ed.). Brunner–Routledge, New York.
[10] J. P. Powell, 1994, *Engineering with Fiber-Polymer Laminates*. Chapman and Hall, London, UK.
[11.] J. N. Reddy, 1997, *Mechanics of Laminated Composite Plates: Theory and Analysis*. CRC Press, Boca Raton, FL.
[12] G. H. Staab, 2015, *Laminar Composites* (2nd ed). Butterworth-Heinemann, Elsevier.
[13] S. W. Tsai, 1992, *Theory of Composites Design*. Think Composites, Dayton, OH.
[14] S. W. Tsai and H. T. Hahn, 2018, *Introduction to Composite Materials*, 2nd ed. CRC, Routledge, Boca Raton, FL.
[15] V. V. Vasiliev and E. V. Morozov, 2018, *Advanced Mechanics of Composite Materials and Structures*. Elsevier, Amsterdam, Netherlands.
[16] G. Z. Voyiadjis and P. I. Kattan, 2005, *Mechanics of Composite Materials with MATLAB*. Springer, Berlin.
[17] T. R. Tauchert, "Piezothermoelastic behavior of a laminated plate," *J. Therm. Stresses*, vol. 15, no. 1, pp. 25–37, 1992. DOI: 10.1080/01495739208946118.
[18] E. Suhir, "Stresses in bi-metal thermostats," *ASME J. Appl. Mech*, vol. 53, no. 3, pp. 657–660, 1986. DOI: 10.1115/1.3171827.

[19] E. Suhir, "An approximate analysis of stresses in multilayered elastic thin films," *ASME J. Appl. Mech*, vol. 55, no. 1, pp. 143–148, 1988. DOI: 10.1115/1.3173620.

[20] E. Suhir, "Interfacial stresses in bimetal thermostats," *ASME J. Appl. Mech*, vol. 56, no. 3, pp. 595–600, 1989. DOI: 10.1115/1.3176133.

[21] Y.-C. Shen and C.-I. Weng, "Deformation control of laminated composite plates containing piezoelectric layers under thermal loading," *J. Therm. Stresses.*, vol. 18, no. 4, pp. 449–464, 1995. DOI: 10.1080/01495739508946313.

[22] E. H. Wong and C. K. Wong, "Tri-layer structures subjected to combined temperature and mechanical loadings," *IEEE Trans. Comp. Packag. Technol*, vol. 31, no. 4, pp. 790–800, 2008. DOI: 10.1109/TCAPT.2008.2001196.

[23] G. Tibi, E. Sachyani, M. Layani, A. Magdassi and A. Degani, 2017. "Analytic modeling and experiments of a tri-layer, electro-thermal actuators for thin and soft robotics," IEEE International Conference on Robotics and Automation, Singapore, May 29–June 3, 2017, pp. 6712–6717.

[24] M. Safaei, H. A. Sodano and S. R. Anton, "A review of energy harvesting using piezoelectric materials: State-of-the-art a decade later (2008–2018)," *Smart Mater. Struct.*, vol. 28, no. 11, pp. 113001–113062, 2019. pages). DOI: 10.1088/1361-665X/ab36e4.

[25] A. Dasgupta, 1991, "Thermo-mechanical analysis and design," In: *Handbook of Electronic Package Design* (M. Pecht, ed.), pp. 477–528. Marcal Dekker, New York.

[26] Pecht, M. (ed.), 1991, *Handbook of Electronic Package Design*. Marcal Dekker, New York.

[27] A. F. Avila and K. K. Tamma, "Integrated micro-macro thermo-elastic-viscoplastic analysis of laminate metal-matrix composites," *J. Therm. Stresses*, vol. 21, no. 9, pp. 897–917, 1998. DOI: 10.1080/01495739808956183.

[28] O. Sayman and S. Sayman, "Thermal elastic-plastic stress analysis of symmetric aluminum metal-matrix composite laminated plates under uniformly distributed temperature," *J. Therm. Stresses*, vol. 25, pp. 363–372, 2002. DOI: 10.1080/014957302753505013.

[29] O. Sayman, "Thermal elastic-plastic stress analysis of symmetric aluminum metal-matrix composite laminated plates under linearly distributed temperature," *J. Therm. Stresses*, vol. 26, pp. 1–12, 2003. DOI: 10.1080/713855761.

[30] X. Zhao and Z. Suo, "Electrostriction in elastic dielectrics undergoing large deformation," *J. Appl. Phys.*, vol. 104, no. 12, pp. 123530, 2008. 7 pages). DOI: 10.1063/1.3031483.

[31] Y. Y. Tang and K. Xu, "Dynamic analysis of a piezothermoelastic laminated plate," *J. Therm. Stresses*, vol. 18, no. 1, pp. 87–104, 1995. DOI: 10.1080/01495739508946292.

[32] N. Dhanesh and S. Santosh Kapuria, "Edge effects in elastic and piezoelectric laminated panels under thermal loading," *J. Therm. Stress.*, vol. 41, no. 10–12, pp. 1577–1596, 2018. DOI: 10.1080/01495739.2018.1524732.

[33] J. N. Reddy, "On laminated composite plates with integrated sensors and actuators," *Eng. Structures*, vol. 21, no. 7, pp. 568–593, 1999. DOI: 10.1016/S0141-0296(97)00212-5.

[34] Z.-Q. Cheng and R. C. Batra, "Three-dimensional asymptotic scheme for piezothermoelastic laminates," *J. Therm. Stress.*, vol. 23, pp. 95–110, 2000.

[35] M. Cinefra, M. Petrolo, G. Li and E. Carrera, "Hygrothermal analysis of multilayered composite plates by variable kinematic finite elements," *J. Therm. Stress.*, vol. 40, no. 12, pp. 1502–1522, 2017. DOI: 10.1080/01495739.2017.1360164.

[36] M. Shojaeifard, M. R. Bayat and M. Baghani, "Swelling-induced finite bending of functionally graded pH-responsive hydrogels: A semi-analytical method," *Appl. Math. Mech.-Engl. Ed*, vol. 40, no. 5, pp. 679–694, 2019. DOI: 10.1007/s10483-019-2478-6.

[37] W.-H. Chu, M. Mehregany and R. L. Mullen, "Analysis of tip deflection and force of a bimetallic cantilever microactuator," *J. Micromech. Microeng.*, vol. 3, no. 1, pp. 4–7, 1993. DOI: 10.1088/0960-1317/3/1/002.

[38] W. T. Chen and C. W. Nelson, "Thermal stresses in bonded joints," *IBM J. Res. Dev.*, vol. 23, no. 2, pp. 179–187, 1979. DOI: 10.1147/rd.232.0179.

[39] D. Chen, S. Cheng and T. D. Gerhardt, "Thermal stresses in laminated beams," *J. Therm. Stress.*, vol. 5, no. 1, pp. 67–84, 1982. DOI: 10.1080/01495738208942136.

[40] Z. Suo and J. W. Hutchinson, "Interface crack between two elastic layers," *Int J Fract*, vol. 43, no. 1, pp. 1–18, 1990. DOI: 10.1007/BF00018123.

[41] Q. Jiang, Y. Huang and A. Chandra, "Thermal stresses in layered electronic assemblies," *ASME J. Electron Packaging*, vol. 119, no. 2, pp. 127–132, 1997. DOI: 10.1115/1.2792218.

[42] W. Xie and S. K. Sitaraman, "Interfacial thermal stress analysis of anisotropic multi-layered electronic packaging structures," *ASME J. Electron. Packag*, vol. 122, no. 1, pp. 61–66, 2000. DOI: 10.1115/1.483133.

[43] Y. Wen and C. Basaran, "An analytical model for thermal stress analysis of multi-layered microelectronic packaging," *Mech. Mater*, vol. 36, no. 4, pp. 369–385, 2004. DOI: 10.1016/S0167-6636(03)00076-0.

[44] M. Lee and I. Jasiuk, "Asymptotic expansions for the thermal stresses in bonded semi-infinite bi-material strips," *ASME J. Electron. Packag*, vol. 113, no. 2, pp. 173–177, 1991. DOI: 10.1115/1.2905383.

[45] J. G. Smits and W.-S. Choi, "The constituent equations of piezoelectric heterogeneous bimorphs," *IEEE Trans. Ultrason. Ferroelectr. Freq. Control.*, vol. 38, no. 3, pp. 256–270, 1991. DOI: 10.1109/58.79611.

[46] G. C. Sih, J. G. Michopoulos and S. C. Chou, 1986, *Hygrothermoelasticity*. M. Nijhoff, Dordrecht.

[47] H. Quan, A. Pirosa, W. Yang, R. O. Ritchie and M. A. Meyers, "Hydration-induced reversible deformation of the pine cone," *Acta Biomater.*, vol. 128, pp. 370–383, 2021. DOI: 10.1016/j.actbio.2021.04.049.

[48] A. Amiri-Hezaveh, P. Karimi and M. Ostoja-Starzewski, "Stress field formulation of linear electro-magneto-elastic materials," *Math. Mech. Solids*, vol. 24, no. 12, pp. 3806–3822, 2019. DOI: 10.1177/1081286519857127.

[49] M. Avellaneda and G. Harshe, "Magnetoelectric effect in piezoelectric/magnetostrictive multilayer (2-2) composites," *J. Intell. Mater. Syst. Struct.*, vol. 5, no. 4, pp. 501–513, 1994. DOI: 10.1177/1045389X9400500406.

[50] D. Hunter, et al., "Giant magnetostriction in annealed Co(1-x)Fe(x) thin-films," *Nat Commun*, vol. 2, pp. 518 (7 pp.), 2011. DOI: 10.1038/ncomms1529.

[51] S. H. Lim, H. J. Kim, S. M. Na and S. J. Suh, "Application-related properties of giant magnetostrictive thin films," *J. Magn. Magn. Mater*, vol. 239, no. 1-3, pp. 546–550, 2002. DOI: 10.1016/S0304-8853(01)00660-6.

[52] A. Ludwig and E. Quandt, "Giant magnetostrictive thin films for applications in microelectromechanical systems," *J. Appl. Physics*, vol. 87, no. 9, pp. 4691–4695, 2000. DOI: 10.1063/1.373132.

[53] S. Manna, *et al.*, "Characterization of strain and its effects on ferromagnetic nickel nanocubes," *AIP Adv.*, vol. 7, no. 12, pp. 125025, 2017. DOI: 10.1063/1.5004577.

[54] C.-W. Nan, M. I. Bichurin, S. Dong, D. Viehland and G. Srinivasan, "Multiferroic magnetoelectric composites: Historical perspective, status, and future directions," *J. Appl. Phys.*, vol. 103, no. 3, pp. 031101, 2008. DOI: 10.1063/1.2836410.

[55] E. Pan, "Exact solution for simply supported and multilayered magneto-electro-elastic plates," *J. Appl. Mech.*, vol. 68, no. 4, pp. 608–618, 2001. DOI: 10.1115/1.1380385.

[56] A. Pateras, et al., "Room temperature giant magnetostriction in single-crystal nickel nanowires," *NPG Asia Mater.*, vol. 11, no. 1, pp. 59–57, 2019. DOI: 10.1038/s41427-019-0160-8.

[57] M. V. Lubarda and V. A. Lubarda, "Recursive formulas for curvature and internal stresses in thermally loaded multilayer strips," *J. Therm. Stresses*, vol. 45, 2022.